Article

Potential Neuroprotective Role of Calretinin-N18 and Calbindin-D28k in the Retina of Adult Zebrafish Exposed to Different Wavelength Lights

Caterina Porcino [1,†], Marilena Briglia [1,†], Marialuisa Aragona [1], Kamel Mhalhel [1], Rosaria Laurà [1], Maria Levanti [1], Francesco Abbate [1], Giuseppe Montalbano [1], Germana Germanà [1], Eugenia Rita Lauriano [2], Alessandro Meduri [3], Josè Antonio Vega [4,5], Antonino Germanà [1,*] and Maria Cristina Guerrera [1]

[1] Zebrafish Neuromorphology Lab, Department of Veterinary Sciences, University of Messina, 98168 Messina, Italy
[2] Department of Chemical, Biological, Pharmaceutical and Environmental Sciences, University of Messina, Viale F. Stagno d'Alcontres 31, 98166 Messina, Italy
[3] Unit of Ophthalmology, Department of Biomedical and Dental Sciences, and of Morphological and Functional Images, University of Messina, 98124 Messina, Italy
[4] Departamento de Morfología y Biología Celular, Grupo SINPOS, Universidad de Oviedo, 33006 Oviedo, Spain
[5] Facultad de Ciencias de la Salud, Universidad Autónoma de Chile, Santiago 7500912, Chile
[*] Correspondence: antonino.germana@unime.it or agermana@unime.it
[†] These authors contributed equally to this work.

Abstract: The incidence rates of light-induced retinopathies have increased significantly in the last decades because of continuous exposure to light from different electronic devices. Recent studies showed that exposure to blue light had been related to the pathogenesis of light-induced retinopathies. However, the pathophysiological mechanisms underlying changes induced by light exposure are not fully known yet. In the present study, the effects of exposure to light at different wavelengths with emission peaks in the blue light range (400–500 nm) on the localization of Calretinin-N18 (CaR-N18) and Calbindin-D28K (CaB-D28K) in adult zebrafish retina are studied using double immunofluorescence with confocal laser microscopy. CaB-D28K and CaR-N18 are two homologous cytosolic calcium-binding proteins (CaBPs) implicated in essential process regulation in central and peripheral nervous systems. CaB-D28K and CaR-N18 distributions are investigated to elucidate their potential role in maintaining retinal homeostasis under distinct light conditions and darkness. The results showed that light influences CaB-D28K and CaR-N18 distribution in the retina of adult zebrafish, suggesting that these CaBPs could be involved in the pathophysiology of retinal damage induced by the short-wavelength visible light spectrum.

Keywords: CaBPs; retina; zebrafish

1. Introduction

The most recent WHO estimates suggest that, in the world, 285 million people suffer from visual disabilities and, of these, 39 million are blind. The prevalence of people affected by blindness and vision impairment is predicted to increase and reach a value of 115 million by 2050 [1,2]. Risk factors predispose to the onset of ocular pathogenesis, among them oxidative stress, vascular changes, and light radiation. This latter can damage the eye through photomechanical, photochemical, and photothermal mechanisms [3,4]. Photochemical retina injury induced by light exposure depends on light wavelength. Short wavelength radiations are the most harmful. In the last few years, human exposure to UV light has increased because of the constant exposure to several electronic devices that emit up to 40% light in the wavelength range between 400 to 490 nanometers, causing irreparable damage to the retina [5]. Cytotoxicity blue light-induced was demonstrated [6],

in particular, photoreceptor injury was observed by Tosini et al. [7]. Light stimuli affect calcium cell concentration [8] and an altered balance of this ion contributes to the appearance of degenerative processes in the retina [9] since calcium is involved in cell development and maturation, synaptogenesis, and maintenance of neuronal circuits in this organ [10,11]. Calcium homeostasis is regulated by calcium-binding proteins (CaBPs), including the EF–hand proteins Calretinin-N18 (CaR-N18) and Calbindin (CaB-D28K). These proteins are widely distributed in central and peripheral nervous systems, including the retina [12–15] where they are employed as neuronal markers [16–22]. CaR-N18 and CaB-D28K are involved in calcium signaling regulating message targeting, intracellular calcium buffering, and neuronal excitability modulation [23–28]. Presumably, CaB-D28K can play a role in retinal disease. However, its precise roles in retinal disease are still unknown and remain the object of further studies. It was suggested that these calcium-binding proteins could also have a protective role in the retina [29]. CaB-D28K has been attributed to a protective role against the horizontal cells and ganglion cells of rats with retinal ischemia. Further, CaBPs can protect against excitotoxicity caused by an increased release of neurotransmitters by regulating the concentration of intracellular calcium [30–39]. Both mammals and fish, including zebrafish (*Danio rerio*), express CaR-N18 and CaB-D28K [40–45]. Zebrafish is commonly used in biomedical research to study human pathologies, including visual disorders [46–49] and photochemical stress, because it shows all the characteristics are considered suitable for scientific research [50,51]. In zebrafish and other vertebrates, the expression of the different CaBPs in the retinal neurons was studied, but their role is still unclear. Moreover, it was never investigated if light exposure could affect CaR-N18 and CaB-D28K distribution in the retina. Therefore, this study intended to compare the immunohistochemical localizations of CaR-N18 and CaB-D28K in the retina of adult zebrafish exposed to different wavelengths of light to understand if light could affect the pattern of distribution of these proteins. Finally, the present study could provide additional information on the potential involvement of CaR-N18 and CaB-D28K in retinal homeostasis maintenance.

2. Results

The zebrafish retina shows an overlapping stratigraphy to mammals, including humans (Figure 1).
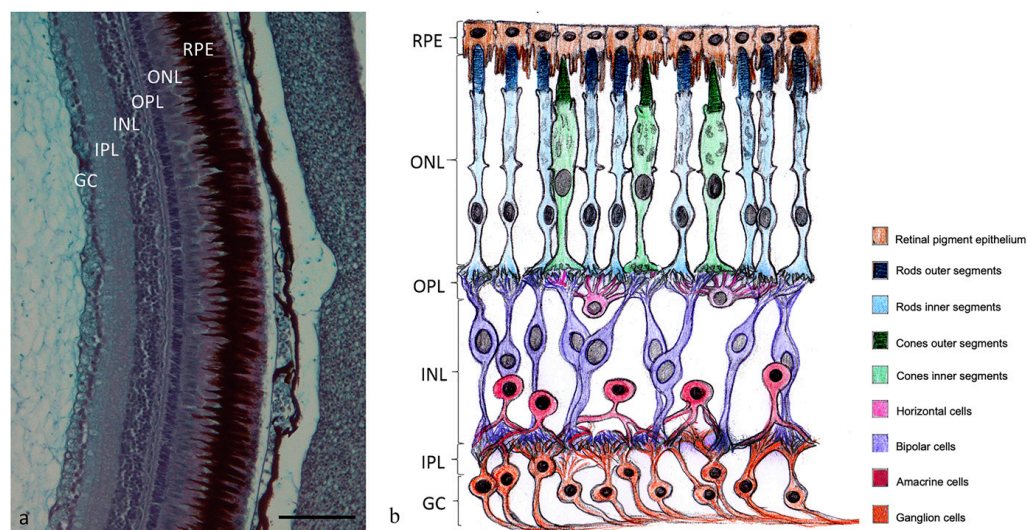

Figure 1. (**a**) Retina of adult zebrafish: RPE, retinal pigment epithelium; ONL, outer nuclear layer; OPL, outer plexiform layer; INL, inner nuclear layer; IPL, inner plexiform layer; GC, ganglion cell layer; Alcian Blue-PAS staining. Magnification 20×. (**b**) Graphical representation of the cell layers into the retina.

The comparison of the immunohistochemical localization of Calbindin (CaB-D28K) and Calretinin (CaR-N18) revealed distinct distribution patterns in the retinal layers in the different experimental groups. In the control group samples (kept in natural photoperiod), retinal pigment epithelium (RPE) showed a CaB-D28K immunoreactivity in the cytoplasmic prolongations of its cells (microvilli). CaB-D28K-immunoreactivity was observed in the photoreceptors layer, both in cones and rods. CaR-N18 immunoreactivity was observed in the outer plexiform layer, in the soma of a subpopulation of amacrine cells and bipolar cells, in the inner plexiform layer (IPL), and in the soma of ganglion cells (GCs) (Figure 2a–c). White light-exposed samples showed a CaB-D28K-immunoreactivity in the RPE cytoplasmatic prolongations and both in the outer and inner segments of cones and rods. A CaB-D28K-immunoreactivity was found in the outer plexiform layer (OPL), in the bipolar cells (BC), in the inner plexiform layer (IPL), and the ganglion cells and their axons (GC). CaR-N18-immunoreactivity was found in the inner segment of cones, in the rods, in the innermost layer of the OPL, in the innermost zone of the IPL, and the ganglion cells and their axons (GC). A CaB-D28K/CaR-N18 colocalization was observed in the inner segments of cones and outer segments of rods, in the IPL, and the GCs and their axons (Figure 2d–f). Sample white–blue light-exposed showed a CaB-D28K-immunoreactivity in the cytoplasmic prolongations of the RPE, in the outer segment of cones, in the rods, in the OPL, in BCs, and in IPL. A CaR-N18 immunoreactivity was found in the inner segment of cones, in the rods, in the innermost of OPL, in the BCs. A low immunoreactivity to CaR-N18 was found in a subpopulation of amacrine cells. Finally, the innermost layer of IPL and GCs and their axons showed CaR-N18 immunoreactivity also. CaB-D28K/CaR-N18 colocalization was found in the inner segment of cones, in the rods, in the innermost layer of the OPL, in the BCs, and in the IPL (Figure 2g–i). A sample exposed to blue light showed CaB-D28K-immunoreactivity in the outer and inner segments of cones and in the rods. A CaB-D28-immunoreactivity was found in the OPL, bipolar cells, some amacrine cells, and ganglion cells and their axons. The inner segments of cones and rods, a subpopulation of amacrine cells, ganglion cells, and their axons were immunoreactive to CaR-N18. CaB-D28K and CaR-N18 were colocalized in the inner segments of cones and in the rods, and in some ganglion cells and their axons (Figure 2j–l). Samples held in darkness showed low CaB-D28K and CaR-N18 immunoreactivity in the photoreceptors layer, but there was no immunoreactivity in the other retinal layers (Figure 2m–o).
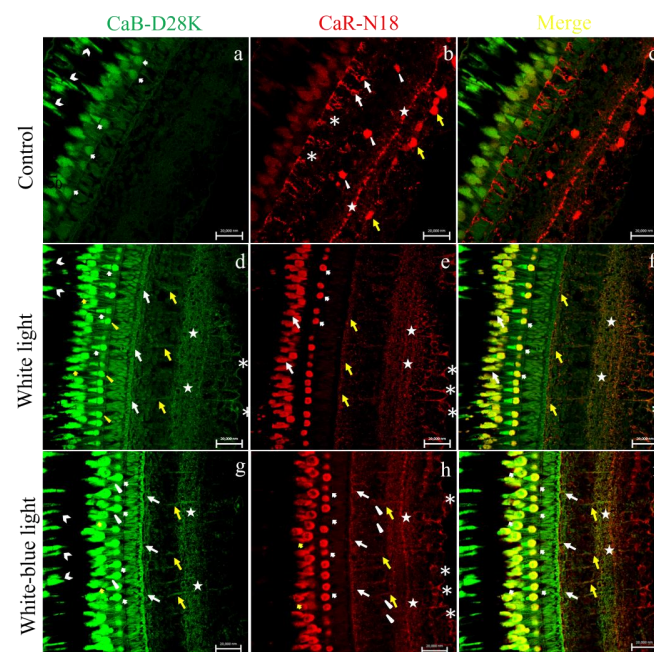

Figure 2. *Cont.*
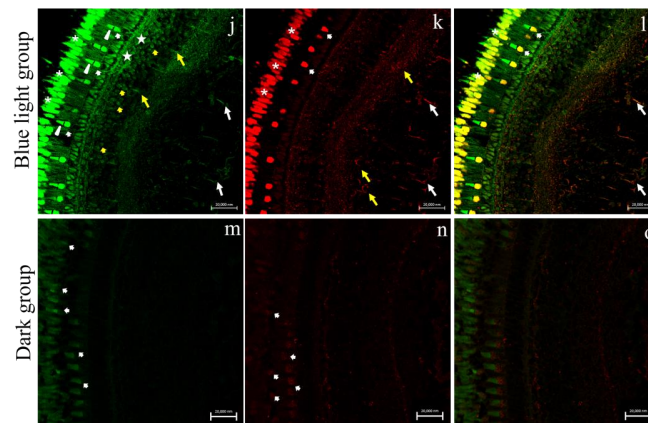
Figure 2. Calbindin-D28K/Calretinin-N18 immunostaining in zebrafish (*Danio rerio*) retina, approximately 4-months-old. (**a**–**c**) Calbindin-D28K/Calretinin-N18 immunostaining in control group (natural photoperiod conditions) (**a**) CaB-D28K-immunoreactivity in the cytoplasmic prolongations of the cells of the retinal pigment epithelium (RPE) (chevron arrows), in the cones and rods of the photoreceptors layer (bold arrows). (**b**) CaR-N18 immunoreactivity in the outer plexiform layer (OPL) (asterisks), in the soma of a subpopulation of amacrine cells (arrowheads) and bipolar cells (arrows), in the inner plexiform layer (IPL) (stars), and in the soma of ganglion cells (GCs) (yellow arrows). (**c**) Merge: absence of Calbindin-D28K/Calretinin-N18 colocalization. (**d**–**f**) Calbindin-D28K/Calretinin-N18 immunostaining in white light group (emission 34.8% of 400–500 nm). (**d**) CaB-D28K-immunoreactivity in the cytoplasmic prolongations of the cells of the retinal pigment epithelium (RPE) (chevron arrows), in the outer segments of cones (bold arrows), and inner segment of cones (yellow arrowheads) and in the rods (yellow bold arrows), in the outer plexiform layer (OPL) (arrows), in the bipolar cells (yellow arrows), in the inner plexiform layer (IPL) (stars), and in the ganglion cells and their axons (GC) (asterisks). (**e**) Calretinin-N18 immunoreactivity in the inner segments of cones (bold arrows), in the rods (arrows), in the innermost layer of the OPL (yellow arrows), in the innermost layer of the IPL (stars) and in the GCs and their axons (asterisks). (**f**) Merge: Calbindin-D28K/Calretinin-N18 colocalization in inner segments of cones (bold arrows), in the rods (arrows), in the innermost layer of IPL (stars) and OPL (yellow arrows) and in the GCs and their axons (asterisks). (**g**–**i**) Calbindin-D28K/Calretinin-N18 immunostaining in white–blue light group (emission 54.6% of 400–500 nm). (**g**) Calbindin-D28K immunoreactivity in retinal pigment epithelium (RPE) into the cytoplasmic prolongations of its cells (chevron arrow), in the inner (bold arrows) and outer segment of cones (arrows heads), in the rods (yellow bold arrows), in the innermost layer of OPL (arrows), in the bipolar cells (yellow arrows) and in the IPL (stars). (**h**) Calretinin-N18 immunoreactivity in the inner segments of cones (bold arrows), in the rods (yellow bold arrows), in the innermost layer of OPL (arrows), in the BCs (yellow arrows), in a subpopulation of amacrine cells (arrowheads), in the innermost layer of OPL (stars), and in the GCs (asterisk). (**i**) Merge: Calbindin-D28K/Calretinin-N18 colocalization in the photoreceptor layer (bold arrows), in the innermost layer of OPL (arrows), in the BCs (yellow arrows) and in the innermost layer of IPL (stars). (**j**–**l**) Calbindin-D28K/Calretinin-N18 immunostaining in blue light group (emission 84.3% of 400–500 nm). (**m**) Calbindin-D28K immunoreactivity in the outer (arrowheads) and inner (bold arrows) segment of cones and in the rods (asterisks), in the OPL (stars), in some amacrine cells (yellow bold arrows), in the BCs (yellow arrows), and GCs (arrows). (**n**) Calretinin-N18 immunoreactivity in the inner segments of cones (bold arrows) and rods (asterisks), in a subpopulation of amacrine cells (yellow arrows), GCs, and their axons (arrows). (**o**) Merge: Calbindin-D28K/Calretinin-N18 colocalization in the inner segments of cones (bold arrows) and in the rods (asterisks) and in some GCs and their axons (arrows). (**m**–**o**) Sample kept in dark conditions. (**m**) Low CaB-D28K immunoreactivity and (**n**) low CaR-N18 immunoreactivity in the photoreceptors layer. No immunostaining to Calbindin-D28K (**a**) and Calretinin-N18 (**b**) in the other retinal layers. (**o**) Merge: no immunostaining to Calbindin-D28K/Calretinin-N18. Magnification 40× (**a**–**o**).

3. Discussion

Despite its peripheral location, the retina or neural portion of the eye is part of the central nervous system, and it is continuously exposed to light radiation. As mentioned above, it is widely recognized that long-term exposure to high-intensity light often causes retinal lesions. It has been demonstrated that short-wavelength visual blue light negatively affects mitochondrial function, causing oxidative stress and decreased cell survival [52,53]. Moreover, Sanchez et al. [54] demonstrated that light regulates the expression of the BDNF and its receptor TrkB in the retina of adult zebrafish under a short-wavelength visible light spectrum. The present study is conducted on adult zebrafish because its retina shows interesting morpho-functional similarities with the human retina. For instance, they share the density of cones and the presents of rods, and light-perception mechanism. Moreover, humans and zebrafish show an overlapping stratigraphy of the retina, consisting of three cell layers interspersed with two synaptic layers [55–58]. For all these reasons, zebrafish turned into a valuable model for studying many vision disorders compared to the more traditional mouse model [59–62]. Calbindin (CaB-D28K) and Calretinin (CaR-N18) are calcium-related proteins in the retina and are mainly distributed in the neuroepithelial layer. Their decrease leads to disorders of calcium-dependent activities. At the same time, the decreased expression of CaB-D28K and CaR-N18 leads to the dysfunction of horizontal, amacrine, and bipolar cells in the retina, reducing visual function [41,63]. With the present investigation, we detect the presence of CaB-D28K in the cytoplasmatic prolongation of the RPE. This is intriguing because this epithelium plays a vital role in keeping rods and cones healthy and well-functioning. The RPE is involved in the absorption of light passing through the neural retina, and it participates in the restoration of photosensitivity of dissociated visual pigments in response to light [64]. In control samples, CaB-D28K and CaR-N18 distribution is similar to their distribution in the human retina. For instance, CaB-D28K is expressed in the cones of both zebrafish and humans [65,66]. On the other hand, CaB-D28K is not expressed in the cones of the retina of the rat and mouse [67]. This could be a piece of evidence confirming the zebrafish suitability as a model organism in retinal disorders studies in translational medicine. Zebrafish, humans, mice, and rats showed CaR-N18-immunoreactivity in a subpopulation of amacrine cells [25,68]. In the zebrafish retina, bipolar cells are CaR-N18-immunoreactive, while in bipolar cells of humans, CaR-N18 is colocalized with CaB-D28K [69,70]. On the contrary, no immunoreactivity to CaR-N18 was found in bipolar cells of mice and rats [25,68]. In the same way as rats and humans, zebrafish show immunoreactivity to CaR-N18 in its ganglion cells [43,68,69,71]. On the contrary, the GCs of mice show no immunoreactivity to CaR-N18 [71]. For a comparison of different species CaB-D28K/CaR-N18 localization in the retina layers, see Table 1. Although the expression of CaB-D28K and CaR-N18 in developing and regenerating zebrafish visual system was previously studied [9], their neuronal distribution after light exposure at different wavelengths has not yet been investigated. Some studies have considered the effects of red light on the localization of these CaBPs in the ischemic retina [72]. Hence, the present study demonstrates, for the first time, that the distribution of these two calcium-binding proteins (CaBPs) changes under distinct wavelength light stimuli and dark conditions.

Table 1. Comparison of different species CaB-D28K/CaR-N18 localization in the retina layers.

	Zebrafish *		Rat		Refs.	Mouse		Ref.	Human		Refs.
	CaB-D28K	CaR-N18	CaB-D28K	CaR-N18		CaB-D28K	CaR-N18		CaB-D28K	CaR-N18	
RPE	+	−		+	[68]				+		[69,70]
PRL	+	−	−	+	[68,73]	−		[74]	+	−	[25,65,67,73,75]
OPL	−	+	+	+	[73,76]	+		[77]	+	−	[73,78]
INL			+	+	[68,73,76,79,80]	+	+	[81,82]	+	+	[20,83]

Table 1. *Cont.*

	Zebrafish *		Rat		Refs.	Mouse		Ref.	Human		Refs.
Bipolar cells	−	+	+	−	[68,84]	−	−	[25]	+	+	[25,73,83]
Amacrine cells	−	+	+	+	[67,73,79,85,86]	+	+	[25,87]	+	+	[25,67,73,83]
IPL	−	+	+	+	[68,73,76,79,80]	−	+	[74,81,82,87]	+	+	[70,83,88]
GCL	−	+	+	+	[67,68,73,76,80, 85,86]	+	+	[25,82,87]	+	+	[25,67,73,75,83]

Retinal pigment epithelium (RPE), photoreceptor layer (PRL), outer plexiform layer (OPL), inner plexiform layer (INL), inner plexiform layer (IPL), ganglion cell layer (GCL). * these data refer to the control group sample of the present study.

3.1. White Light Experimental Group versus Control

Compared to the control, the white-light experimental group showed CaR-N18-immunoreactivity in the inner segment of cones and in the rods in colocalization with CaB-D28K (Figure 3a) that is also localized in the RPE, in the outer segments of cones, and in the outer plexiform layer. Moreover, in contrast to the control group, CaB-D28K immunopositivity was observed in the IPL, bipolar cells, and ganglion cells. CaR-N18-immunoreactivity was not found in the amacrine cells of the samples exposed to white light, contrary to what was detected in the control group samples. CaB-D28K-immunoreactivity was found in the outer plexiform layer, in the inner plexiform layer, contrary to what was detected in the control group samples, and in the ganglion cells in colocalization with CaR-N18.
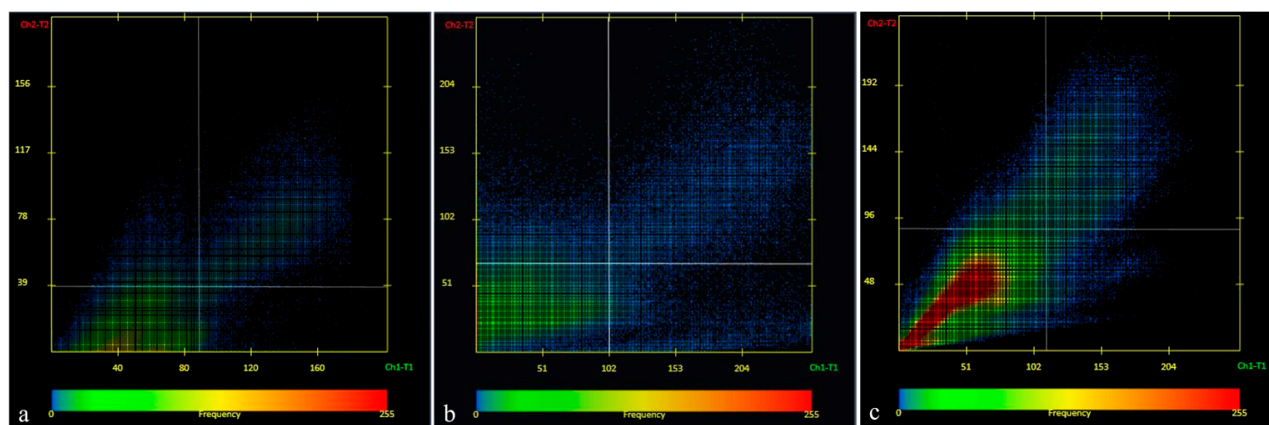

Figure 3. Scatter plot of CaB-D28K/CaR-N18 colocalization in different experimental groups: (**a**) white-light experimental group; (**b**) white/blue-light experimental group; (**c**) blue-light experimental group. Zen 2011 (LSM 700 Zeiss software, Germany).

3.2. White–Blue Light Experimental Group versus Control

In the same way as the control group, CaB-D28K is localized in the RPE of the white–blue light exposed sample. In this experimental group, a CaB-D28K and CaR-N18 colocalization was observed in the inner segment of cones (Figure 3b) and in the rods, whereas, in the control group, CaB-D28K was expressed alone in the inner segments of the rods and the inner and outer segments of the cones. In contrast to the control group, CaB-D28K was found in OPL, bipolar cells, and the IPL. Moreover, CaB-D28K-immunoreactivity appeared in colocalization to CaR-N18 in the OPL, bipolar cell, and IPL of the sample of this experimental group. On the contrary, bipolar cells were immunoreactive only to CaR-N18 in the control group. The CaR-N18-immunoreactivity of the OPL and IPL of the control group samples was also found in the OPL and IPL of the white–blue light-exposed samples. In comparison to the control, CaR-N18-immunoreactivity remained unchanged in ganglion

cells. Amacrine cells of white–blue light exposed samples showed an immunoreactive to CaR-N18 but were lower than the control group.

3.3. Blue Light Experimental Group versus Control

In blue light-exposed samples, the CaB-D28K immunoreactivity is absent in the RPE, unlike the control samples. In this experimental group, CaR-N18 immunoreactivity appeared in colocalization with CaB-D28K in the inner segment of cones and in the rods (Figure 3c). Contrary to the control, CaB-D28K immunoreactivity was observed in OPL, bipolar cells, amacrine cells, and ganglion cells, and no CaR-N18-immunoreactivity was observed in the OPL of the sample of the experimental group. If on one hand CaR-N18 immunoreactivity remained unchanged with respect to control in amacrine and GCs of this experimental group, on the other, it disappeared in bipolar cells and IPL. This experimental group differs from the control one for the CaB-D28K/CaR-N18 colocalization in the GCs. Some authors assume that CaR-N18 has neuronal protection function because it is not expressed when visual system damage occurs [9]. This evidence could be related to the shutdown of the CaR-N18 fluorescent signal in the OPL and IPL of our blue-light experimental group.

3.4. Darkness Experimental Group versus Control

It is now well-established that light stimulation is essential for vertebrate retina maintenance during adulthood [89–91]. Hence, it could be speculated that long-term exposure to darkness made the retina of the samples of this experimental group less responsive to light, especially after a prolonged period (10 days). From a biochemical point of view, a possible explanation for the weakening of the fluorescent signal in photoreceptors and the lack of expression on the other retinal layer could be that darkness acts by inducing a release of inhibitory neurotransmitter and a block of Ca^{2+} in the storage site, so CaBPs presence is unnecessary. On the other hand, the localization of CaB-D28K in the cones of the samples held in the dark could be related to the nature of these photoreceptors involved in nocturnal vision mechanisms.

3.5. Comparison between the Distinct Experimental Groups

What emerges from our observations is that artificial light affects CaB-D28K and CaR-N18 distribution in the different retinal layers, regardless of the light wavelengths. As a matter of fact, the statistical analysis shows a different distribution pattern of the two proteins between the experimental groups compared to the control (natural photoperiod) (Figure 4 and Table 2). It is recognized that EF–hand CaBPs are involved in homeostasis and neuroprotection thanks to their Ca^{2+} buffering properties [8]. Therefore, the different distribution patterns of CaB-D28K and CaR-N18 could be related to an increased Ca^{2+} concentration in retinal cells due to the light stimuli. What is reported in the literature is that Calretinin-immunoreactivity changes in some pathological conditions of the retina, for instance, in amacrine cells [92]. This pattern is shared with the sample kept in white, white–blue, and dark conditions during our experimentation. A recurring trend regards the localization of Calbindin in the OPL of the retina of all artificial light-exposed animals. Considering that the neuroprotective role of Calbindin is recognized by some members of the scientific community [8,93], this trend could be interpreted as a response of some cells to protect themselves from excessive excitability induced by chronic exposure to different artificial lights. In the same way, Calbindin appears in all the bipolar cells of fish exposed to artificial light. Another recurring trend is the appearance of Calretinin in the cones and rods of the samples exposed to all the lights.
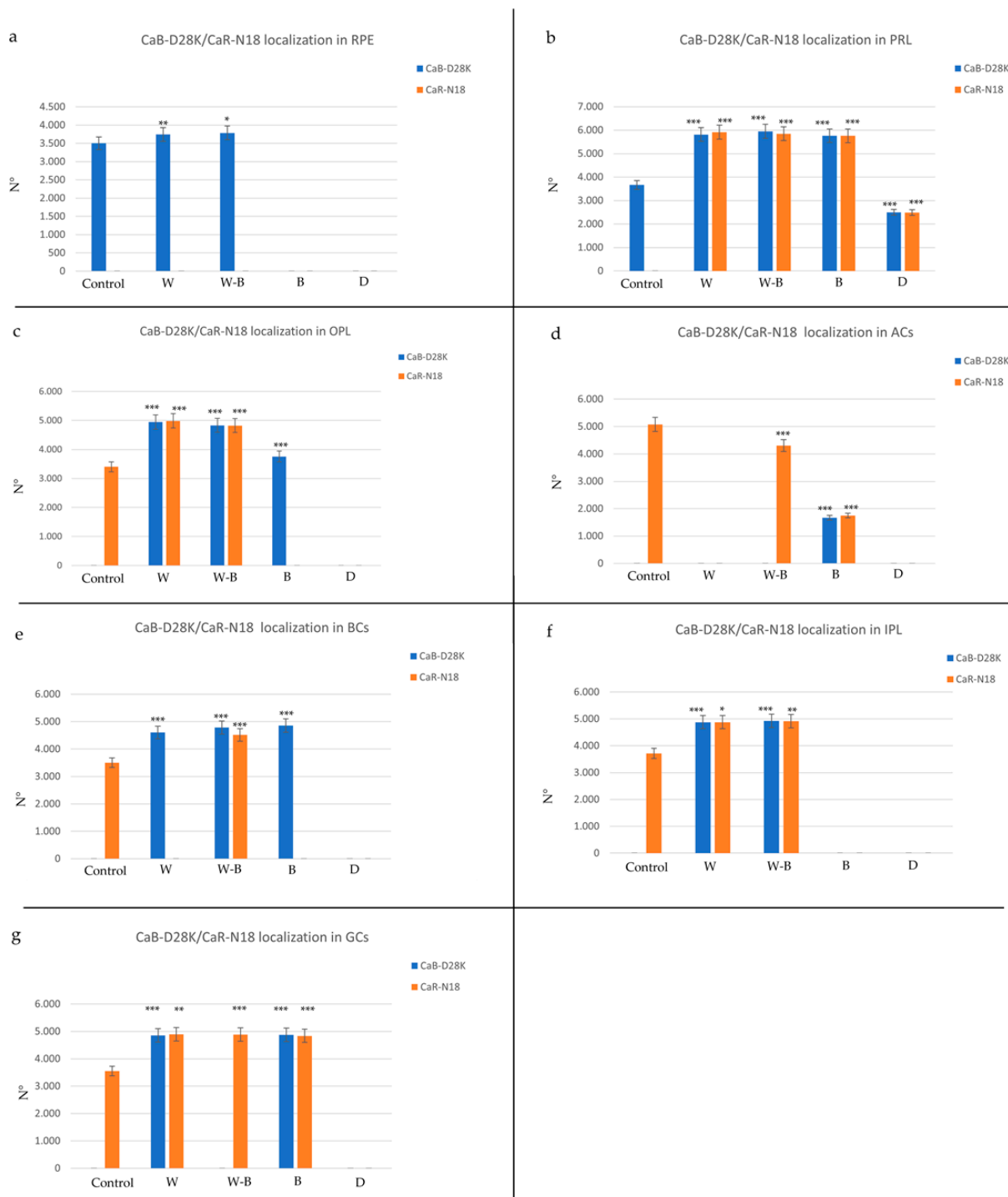
Figure 4. Graphical representation of immunopositivity of: (**a**) retinal pigment epithelium (RPE), (**b**) photoreceptor layer (PRL), (**c**) outer plexiform layer (OPL), (**d**) amacrine cells (ACs), (**e**) inner plexiform layer (IPL), (**f**) bipolar cells (BCs), (**g**) ganglion cells (GCs) detected by Calbindin (CaB-D28K) and Calretinin (CaR-18N) in different experimental groups. Experimental conditions: control (natural photoperiod), white light with a 34.8% of blue light emission (W), white–blue light with a 54.6% of blue light emission (WB), blue light with an 84.3% of blue light emission (B) and darkness (D). The statistical analysis shows a different distribution pattern of the two proteins between the experimental groups compared to the control. Data represent the average of measurements from the ten sections from each treatment. Statistical significance: *** $p < 0.001$, ** $p < 0.01$, * $p < 0.05$.

Table 2. Mean data ± standard deviation (Δσ) of immunopositivity of: GC (ganglion cell); IPL (inner plexiform layer); INL (inner nuclear layer); OPL (outer plexiform layer); ONL (outer nuclear layer); RPE (retinal pigment epithelium) detected by Calbindin (CaB-D28K) and Calretinin (CaR-18N). Experimental conditions: control (natural photoperiod), white light with a 34.8% of blue light emission (W), white–blue light with a 54.6% of blue light emission (WB), blue light with an 84.3% of blue light emission (B), and darkness (D). The statistical analysis shows a different distribution pattern of the two proteins between the experimental groups compared to the control. All features were evaluated per 174.286 ± 3.082 μm (mean). Statistical significance: *** $p < 0.001$, ** $p < 0.01$, * $p < 0.05$.

Treatment	Mean ± Δσ in RPE		Mean ± Δσ in PRL		Mean ± Δσ in OPL		Mean ± Δσ of Amacrine Cells		Mean ± Δσ of Bipolar Cells		Mean ± Δσ in IPL		Mean ± Δσ of Ganglial Cells	
	CaB-D28K	CaR-N18	CaB-D28K	CaR-N18	CaB-D28K	CaR-N18	CaB-D28K	CaR-N18	CaB-D28K	CaR-N18	CaB-D28K	CaR-N18	CaB-D28K	CaR-N18
Control	3.503 ± 0.45	-	3.663 ± 0.73		-	3.403 ± 0.54	-	5.076 ± 0.66	-	3.503 ± 0.45	-	3.713 ± 0.58	-	3.553 ± 0.47
White	3.743 ± 0.30 **	-	5.810 ± 1.33 ***	5.910 ± 1.39 ***	4.946 ± 2.11 ***	4.986 ± 2.15 ***	-	-	4.602 ± 0.85 ***	-	4.876 ± 1.74 ***	4.876 ± 1.74 *	4.855 ± 1.73 ***	4.894 ± 1.52 **
White–Blue	3.786 ± 0.41 *	-	5.944 ± 1.42 ***	5.844 ± 1.34 ***	4.833 ± 1.37 ***	4.824 ± 1.36 ***	-	4.303 ± 0.66 ***	4.782 ± 0.62 ***	4.513 ± 0.58 ***	4.924 ± 1.51 ***	4.915 ± 1.26 **	-	4.888 ± 0.88 ***
Blue	-	-	5.755 ± 0.95 ***	5.515 ± 0.95 ***	3.758 ± 0.29 ***	-	1.668 ± 0.40 ***	1.746 ± 0.39 ***	4.855 ± 1.73 ***	-	-	-	4.874 ± 0.48 ***	4.838 ± 0.65 ***
Dark	-	-	2.500 ± 1.06 ***	2.485 ± 0.42 ***	-	-	-	-	-	-	-	-	-	-

4. Materials and Methods

4.1. Experimental Protocol

For this study, twenty adult zebrafish paraffin, embedded for previous experimentation, were used (see Sánchez Ramos et al. [54]). In that experiment, the groups were exposed to white light, white–blue light, blue light, and darkness, respectively, while the fishes of the control group were kept in natural photoperiod conditions. Experimental conditions had been maintained continuously for 10 days for all groups [54]. Fish have been maintained at 28 °C using standard conditions in different transparent plastic tanks. Light sources were placed 3 cm above the tank (for illumination source details, see Table 3 and Figure 5). Furthermore, a group of fish was exposed to darkness in a special black tank. The characteristics of each type of light, to which different experimental groups were exposed, were determined by the Department of Optics II, Universidad Complutense, Madrid, Spain. They were chosen to investigate the effects of the different percentages of blue light content. Four specimens for each of the five experimental groups were employed. The included tissue samples were then cut into 7 μm thick serial sections and collected on gelatin-coated microscope slides [94–97]. Some sections were deparaffinized and rehydrated, washed in distilled water, and stained with Alcian Blue pH 2.5 Periodic Acid Schiff (AB/PAS) (04-163802, Bio-Optica Milano S.p.a., Milan, Italy). Sections were examined under an OLYMPUS BX51 system Microscope (Olympus Optical Co., Ltd., Nagano, Japan), and micrographs were taken using a digital camera OLYMPUS DP12 (Olympus Optical Co., Ltd., Nagano, Japan).

Table 3. Illumination source details. Irradiancies were measured using a photoradiometric TektronixJ1800 (TekLumaColor, Wilsonville, OR, USA). The spectral composition of the light source was determined using the optic fiber spectrophotometer Spectrawiz EPP2000 (StellarNet, Keystone, FL, USA).

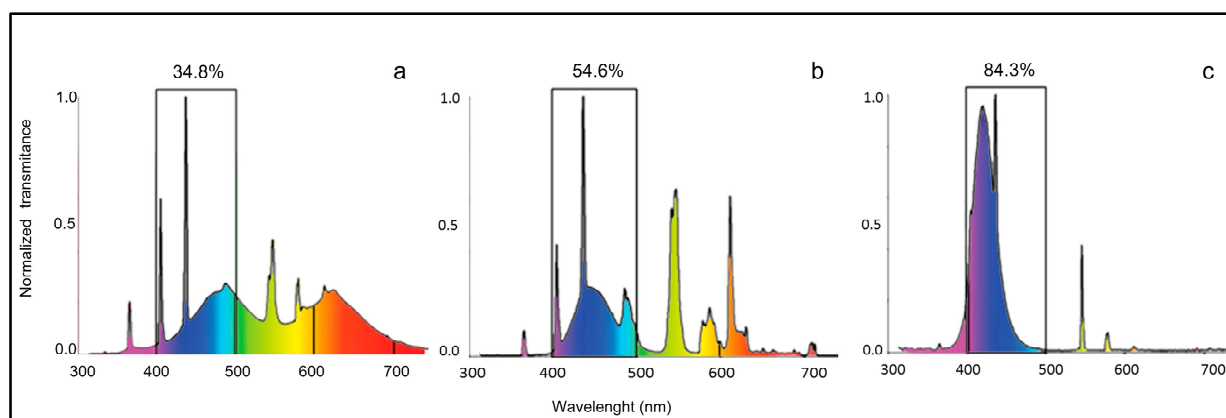|	White Light	White–Blue Light	Blue Light
Source	Philips MASTER TL-D Reflex 18W/840	RADIUM NL 18W/965 Biosun	Philips TL 20W/03 RS 1SL
Light	T^a 4.000 °K	T^a 6.500 °K	TL 20W/03 RS 1SL
Manufacturer	Philips, Consumer Lifestyle, Spain	Radium Lampenwerk GmbH, Germany	Philips, Consumer Lifestyle, Spain
Emission	34.8% of 400–500 nm	54.6% of 400–500 nm	84.3% of 400–500 nm
Irradiation	28.57 W/m^2	93.46 W/m^2	27.85 W/m^2

Figure 5. Spectral distribution of the illumination sources. (**a**) white light, (**b**) white–blue light, (**c**) blue light. The percentage of blue light emission for each experiment is indicated.

4.2. Confocal Immunofluorescence

To analyze the expression of different proteins in zebrafish retina tissue, sections were deparaffinized and rehydrated, washed in Phosphate-Buffered Saline (PBS) 0.1 M pH = 7.4, and incubated in 0.3% H_2O_2 (PBS) solution for 3 min to prevent the activity of endogenous peroxidase; then, to rinsed sections, fetal bovine serum was added (F7524 Sigma-Aldrich, St. Louis, MO, USA). Calretinin goat antibody (N18-sc-11644 Santa Cruz Biotechnology, Santa Cruz, CA, USA) was used in double-label experiments with a monoclonal antibody to Anti-Calbindin-D28K (C9848 Sigma-Aldrich). Both the employed antibodies were diluted 1:100. Sections were incubated overnight at 4 °C in a humid chamber with antibodies. The specificity of the antibodies has been previously tested in zebrafish [13,98–100]. After rinsing in PBS, the sections were incubated for 1 h at 4 °C with Donkey anti-Goat IgG (H+L) Alexa Fluor 594 (Invitrogen A-11058, Waltham, MA, USA, 1:100); Donkey anti-Mouse IgG (H+L) Alexa Fluor 488 (Invitrogen A-21202 1:100). Both steps were performed at room temperature in a dark humid chamber. Finally, the section was washed and mounted with Fluoromount Aqueous Mounting Medium (Sigma Aldrich, USA) to prevent photobleaching, and then they were cover-slipped. To provide negative controls, representative sections were incubated with specifically preabsorbed antisera as described above. Under these conditions, no positive immunostaining was observed.

The immunofluorescence was detected using a Zeiss LSMDUO confocal laser scanning microscope with META module (Carl Zeiss Micro Imaging GmbH, Göttingen, Germany) microscope LSM700 AxioObserver. Zen 2011 (LSM 700 Zeiss software) built-in "colocalization view" was used to highlight the expression of both antibodies signals in order to produce a "colocalization" signal, the scatter plot, and fluorescent signal measurements. Each image was rapidly acquired to minimize photodegradation.

4.3. Statistical Analysis

ImageJ software was used to evaluate microscope fields collected randomly. One-way ANOVA was used to examine the statistical significance of the quantity of retinal pigment epithelium (RPE), photoreceptor layer (PRL), outer plexiform layer (OPL), amacrine cells (ACs), inner plexiform layer (IPL), bipolar cells (BCs), ganglion cells (GCs) detected by CaB-D28K, and CaR-18N in different experimental conditions. SigmaPlot version 14.0 (Systat Software, San Jose, CA, USA) was used to conduct the statistical analysis. An unpaired Z test was also performed. The information was given as median values with standard deviations ($\Delta\sigma$). Values of *p* below 0.05 were considered statistically significant in the following order *** $p < 0.001$, ** $p < 0.01$, * $p < 0.05$.

5. Conclusions

The present study demonstrates that light regulates Calbindin (CaB-D28K) and Calretinin (CaR-N18) distribution in the retina of adult zebrafish. It suggests that these calcium-binding proteins (CaBPs) could be involved in the pathophysiology of short-wavelength visible light spectrum retinal damage. However, it remains to be elucidated if the expression of Calbindin and Calretinin in cells where usually they are not expressed (and vice versa their silencing) could be intended as a protective response to light or if light-induced damage occurs through an altered localization of these two calcium-binding proteins. This kind of understanding could represent a starting point for future studies on phototoxicity, and retinal degeneration. To investigate the potential therapeutic role of CaBPs in the treatment of light-induced retinal damage, further studies are needed to elucidate the function of CaR-N18 and CaB-D28K in the recovery of normal conditions after retinal injury due to exposure to UV light and their role in ocular pathogenesis. In our laboratory, ultrastructural analysis of light-induced injury is underway in the adult zebrafish retina as a model for human ocular disorders. Finally, it is necessary to bring new knowledge to CaB-D28K and CaR-N18 role in retinal homeostasis to elucidate their potential role as markers of retinal damage for transversal studies. The findings of the present study demonstrate that CaBPs could be involved in the protection of neurons from light-induced neurodegeneration.

Author Contributions: Conceptualization, A.G. and M.C.G.; methodology, M.A., C.P., M.B. and K.M.; software, M.A., C.P., M.B. and K.M.; validation, A.G., J.A.V., F.A., R.L., M.L., A.M., E.R.L., M.C.G. and G.G.; formal analysis, M.A., C.P., M.B. and K.M.; investigation, M.A., M.C.G., G.M., A.M. and G.G.; resources, A.G., M.C.G. and G.M.; data curation, M.A., M.C.G., G.M. and G.G.; writing—original draft preparation, A.G., J.A.V., M.C.G., M.A., C.P. and M.B.; writing—review and editing, A.G., J.A.V., M.C.G., M.A., C.P., M.B. and E.R.L.; visualization, A.G., J.A.V., F.A., R.L. and M.L.; supervision, A.G., J.A.V., F.A., R.L., M.L., G.G., G.M. and M.C.G.; project administration, A.G. and M.C.G.; funding acquisition, A.G., M.C.G. and G.M. All authors have read and agreed to the published version of the manuscript.

Institutional Review Board Statement: This study has been conducted on paraffin embedded samples of a previous experiment [54].

Data Availability Statement: All data presented this study are available from the corresponding author, upon responsible request.

Conflicts of Interest: The authors declare no conflict of interest.

References

1. Bourne, R.; Steinmetz, J.D.; Flaxman, S.; Briant, P.S.; Taylor, H.R.; Resnikoff, S.; Casson, R.J.; Abdoli, A.; Abu-Gharbieh, E.; Afshin, A.; et al. Trends in prevalence of blindness and distance and near vision impairment over 30 years: An analysis for the Global Burden of Disease Study. *Lancet Glob. Health* **2021**, *9*, e130–e143. [CrossRef] [PubMed]
2. Executive, B. *Draft Action Plan for the Prevention of AVOIDABLE blindness and Visual Impairment 2014–2019: Universal Eye Health: A Global Action Plan 2014–2019: Report by the Secretariat*; World Health Organization: Geneva, Switzerland, 2013.
3. Mainster, M.A.; Turner, P.L. Blue-blocking IOLs Decrease Photoreception without Providing Significant Photoprotection. *Surv. Ophthalmol.* **2010**, *55*, 272–283. [CrossRef] [PubMed]

4. Mainster, M.A.; Turner, P.L. Ultraviolet-B Phototoxicity and Hypothetical Photomelanomagenesis: Intraocular and Crystalline Lens Photoprotection. *Am. J. Ophthalmol.* **2010**, *149*, 543–549. [CrossRef]

5. Arjmandi, N.; Mortazavi, G.; Zarei, S.; Faraz, M.; Mortazavi, S.A.R. Can Light Emitted from Smartphone Screens and Taking Selfies Cause Premature Aging and Wrinkles? *J. Biomed. Phys. Eng.* **2018**, *8*, 447–452. [CrossRef] [PubMed]

6. Ratnayake, K.; Payton, J.L.; Lakmal, O.H.; Karunarathne, A. Blue light excited retinal intercepts cellular signaling. *Sci. Rep.* **2018**, *8*, 10207. [CrossRef]

7. Tosini, G.; Ferguson, I.; Tsubota, K. Effects of blue light on the circadian system and eye physiology. *Mol. Vis.* **2016**, *22*, 61–72.

8. D'Orlando, C.; Celio, M.R.; Schwaller, B. Calretinin and calbindin D-28k, but not parvalbumin protect against glutamate-induced delayed excitotoxicity in transfected N18–RE 105 neuroblastoma–retina hybrid cells. *Brain Res.* **2002**, *945*, 181–190. [CrossRef]

9. García-Crespo, D.; Vecino, E. Differential expression of calretinin in the developing and regenerating zebrafish visual system. *Histol. Histopathol.* **2004**, *19*, 1193–1199.

10. Greer, P.L.; Greenberg, M.E. From Synapse to Nucleus: Calcium-Dependent Gene Transcription in the Control of Synapse Development and Function. *Neuron* **2008**, *59*, 846–860. [CrossRef]

11. Raju, C.S.; Spatazza, J.; Stanco, A.; Larimer, P.; Sorrells, S.F.; Kelley, K.W.; Nicholas, C.R.; Paredes, M.F.; Lui, J.H.; Hasenstaub, A.R.; et al. Secretagogin is Expressed by Developing Neocortical GABAergic Neurons in Humans but not Mice and Increases Neurite Arbor Size and Complexity. *Cereb. Cortex* **2018**, *28*, 1946–1958. [CrossRef]

12. Castro, A.; Becerra, M.; Manso, M.J.; Anadón, R. Calretinin immunoreactivity in the brain of the zebrafish, Danio rerio: Distribution and comparison with some neuropeptides and neurotransmitter-synthesizing enzymes. I. Olfactory organ and forebrain. *J. Comp. Neurol.* **2006**, *494*, 435–459. [CrossRef] [PubMed]

13. Germanà, A.; Paruta, S.; Germanà, G.P.; Ochoa-Erena, F.J.; Montalbano, G.; Cobo, J.; Vega, J.A. Differential distribution of S100 protein and calretinin in mechanosensory and chemosensory cells of adult zebrafish (*Danio rerio*). *Brain Res.* **2007**, *1162*, 48–55. [CrossRef]

14. Castro, A.; Becerra, M.; Anadón, R.; Manso, M.J. Distribution of calretinin during development of the olfactory system in the brown trout, *Salmo trutta* fario: Comparison with other immunohistochemical markers. *J. Chem. Neuroanat.* **2008**, *35*, 306–316. [CrossRef] [PubMed]

15. Levanti, M.B.; Montalbano, G.; Laurà, R.; Ciriaco, E.; Cobo, T.; García-Suarez, O.; Germanà, A.; Vega, J.A. Calretinin in the peripheral nervous system of the adult zebrafish. *J. Anat.* **2008**, *212*, 67–71. [CrossRef]

16. Chin, D.; Means, A.R. Calmodulin: A prototypical calcium sensor. *Trends Cell Biol.* **2000**, *10*, 322–328. [CrossRef] [PubMed]

17. Germana, A.; González-Martínez, T.; Catania, S.; Laura, R.; Cobo, J.; Ciriaco, E.; Vega, J. Neurotrophin receptors in taste buds of adult zebrafish (*Danio rerio*). *Neurosci. Lett.* **2004**, *354*, 189–192. [CrossRef] [PubMed]

18. Germanà, A.; Marino, F.; Guerrera, M.C.; Campo, S.; de Girolamo, P.; Montalbano, G.; Germanà, G.P.; Ochoa-Erena, F.J.; Ciriaco, E.; Vega, J.A. Expression and distribution of S100 protein in the nervous system of the adult zebrafish (*Danio rerio*). *Microsc. Res. Tech.* **2008**, *71*, 248–255. [CrossRef]

19. Parisi, V.; Guerrera, M.C.; Abbate, F.; Garcia-Suarez, O.; Viña, E.; Vega, J.A.; Germanà, A. Immunohistochemical characterization of the crypt neurons in the olfactory epithelium of adult zebrafish. *Ann. Anat.-Anat. Anz.* **2014**, *196*, 178–182. [CrossRef]

20. Kántor, O.; Mezey, S.; Adeghate, J.; Naumann, A.; Nitschke, R.; Énzsöly, A.; Szabó, A.; Lukáts, Á.; Németh, J.; Somogyvári, Z.; et al. Calcium buffer proteins are specific markers of human retinal neurons. *Cell Tissue Res.* **2016**, *365*, 29–50. [CrossRef]

21. Andressen, C.; Blümcke, I.; Celio, M.R. Calcium-binding proteins: Selective markers of nerve cells. *Cell Tissue Res.* **1993**, *271*, 181–208. [CrossRef]

22. Schwaller, B. The use of transgenic mouse models to reveal the functions of Ca^{2+} buffer proteins in excitable cells. *Biochim. et Biophys. Acta (BBA)—Gen. Subj.* **2012**, *1820*, 1294–1303. [CrossRef]

23. Airaksinen, M.S.; Thoenen, H.; Meyer, M. Vulnerability of Midbrain Dopaminergic Neurons in Calbindin-D28k-deficient Mice: Lack of Evidence for a Neuroprotective Role of Endogenous Calbindin in MPTPtreated and Weaver Mice. *Eur. J. Neurosci.* **1997**, *9*, 120–127. [CrossRef] [PubMed]

24. Camp, A.J.; Wijesinghe, R. Calretinin: Modulator of neuronal excitability. *Int. J. Biochem. Cell Biol.* **2009**, *41*, 2118–2121. [CrossRef] [PubMed]

25. Kovács-Öller, T.; Szarka, G.; Ganczer, A.; Tengölics, Á.; Balogh, B.; Völgyi, B. Expression of Ca(2+)-Binding Buffer Proteins in the Human and Mouse Retinal Neurons. *Int. J. Mol. Sci.* **2019**, *20*, 2229. [CrossRef] [PubMed]

26. Jung, E.-M.; An, B.-S.; Choi, K.-C.; Jeung, E.-B. Apoptosis- and endoplasmic reticulum stress-related genes were regulated by estrogen and progesterone in the uteri of calbindin-D9k and -D28k knockout mice. *J. Cell. Biochem.* **2012**, *113*, 194–203. [CrossRef]

27. Fosser, N.S.; Ronco, L.; Bejarano, A.; Paganelli, A.R.; Ríos, H. Calbindin-D28k and calretinin in chicken inner retina during postnatal development and neuroplasticity by dim red light. *Dev. Neurobiol.* **2013**, *73*, 530–542. [CrossRef]

28. Van Hook, M.J.; Thoreson, W.B. Molecular Mechanisms of Photoreceptor Synaptic Transmission. In *Vertebrate Photoreceptors: Functional Molecular Bases*; Furukawa, T., Hurley, J.B., Kawamura, S., Eds.; Springer: Tokyo, Japan, 2014; pp. 167–198. [CrossRef]

29. van Kuyck, K.; Gabriëls, L.; Nuttin, B. Chapter 55—Electrical Brain Stimulation in Treatment-Resistant Obsessive–Compulsive Disorder: Parcellation, and Cyto- and Chemoarchitecture of the Bed Nucleus of the Stria Terminalis—A Review. In *Neuromodulation*; Krames, E.S., Peckham, P.H., Rezai, A.R., Eds.; Academic Press: San Diego, CA, USA, 2009; pp. 677–687. [CrossRef]

30. Miller, R.J. Regulation of calcium homoeostasis in neurons: The role of calcium-binding proteins. *Biochem. Soc. Trans.* **1995**, *23*, 629–632. [CrossRef]

31. Lohmann, C.; Friauf, E. Distribution of the calcium-binding proteins parvalbumin and calretinin in the auditory brainstem of adult and developing rats. *J. Comp. Neurol.* **1996**, *367*, 90–109. [CrossRef]

32. Lukas, W.; Jones, K.A. Cortical neurons containing calretinin are selectively resistant to calcium overload and excitotoxicity in vitro. *Neuroscience* **1994**, *61*, 307–316. [CrossRef]

33. Pike, C.J.; Cotman, C.W. Calretinin-immunoreactive neurons are resistant to β-amyloid toxicity in vitro. *Brain Res.* **1995**, *671*, 293–298. [CrossRef]

34. D'Orlando, C.; Fellay, B.t.; Schwaller, B.; Salicio, V.; Bloc, A.; Gotzos, V.; Celio, M.R. Calretinin and calbindin D-28k delay the onset of cell death after excitotoxic stimulation in transfected P19 cells. *Brain Res.* **2001**, *909*, 145–158. [CrossRef] [PubMed]

35. Kim, S.A.; Jung, C.K.; Kang, T.-H.; Jeon, J.H.; Cha, J.; Kim, I.-B.; Chun, M.-H. Synaptic connections of calbindin-immunoreactive cone bipolar cells in the inner plexiform layer of rabbit retina. *Cell Tissue Res.* **2010**, *339*, 311–320. [CrossRef] [PubMed]

36. Park, H.-S.; Park, S.-J.; Park, S.-H.; Chun, M.-H.; Oh, S.-J. Shifting of parvalbumin expression in the rat retina in experimentally induced diabetes. *Acta Neuropathol.* **2008**, *115*, 241–248. [CrossRef]

37. Hernandez, M.; Rodriguez, F.D.; Sharma, S.C.; Vecino, E. Immunohistochemical changes in rat retinas at various time periods of elevated intraocular pressure. *Mol. Vis.* **2009**, *15*, 2696–2709. [PubMed]

38. Gunn, D.J.; Gole, G.A.; Barnett, N.L. Specific amacrine cell changes in an induced mouse model of glaucoma. *Clin. Exp. Ophthalmol.* **2011**, *39*, 555–563. [CrossRef] [PubMed]

39. Huang, J.-F.; Shang, L.; Zhang, M.-Q.; Wang, H.; Chen, D.; Tong, J.-B.; Huang, H.; Yan, X.-X.; Zeng, L.-P.; Xiong, K. Differential neuronal expression of receptor interacting protein 3 in rat retina: Involvement in ischemic stress response. *BMC Neurosci.* **2013**, *14*, 16. [CrossRef] [PubMed]

40. Pasteels, B.; Rogers, J.; Blachier, F.; Pochet, R. Calbindin and calretinin localization in retina from different species. *Vis. Neurosci.* **1990**, *5*, 1–16. [CrossRef] [PubMed]

41. Massey, S.C.; Mills, S.L. A calbindin-immunoreactive cone bipolar cell type in the rabbit retina. *J. Comp. Neurol.* **1996**, *366*, 15–33. [CrossRef]

42. Kim, D.-J.; Seok, S.-H.; Baek, M.-W.; Lee, H.-Y.; Na, Y.-R.; Park, S.-H.; Lee, H.-K.; Dutta, N.K.; Kawakami, K.; Park, J.-H. Developmental toxicity and brain aromatase induction by high genistein concentrations in zebrafish embryos. *Toxicol. Mech. Methods* **2009**, *19*, 251–256. [CrossRef]

43. Schwaller, B. Cytosolic Ca^{2+} buffers. *Cold Spring Harb. Lab.* **2010**, *2*, a004051. [CrossRef]

44. Kántor, O.; Benkő, Z.; Énzsöly, A.; Dávid, C.; Naumann, A.; Nitschke, R.; Szabó, A.; Pálfi, E.; Orbán, J.; Nyitrai, M.; et al. Characterization of connexin36 gap junctions in the human outer retina. *Brain Struct. Funct.* **2016**, *221*, 2963–2984. [CrossRef] [PubMed]

45. Kovács-Öller, T.; Debertin, G.; Balogh, M.; Ganczer, A.; Orbán, J.; Nyitrai, M.; Balogh, L.; Kántor, O.; Völgyi, B. Connexin36 expression in the mammalian retina: A multiple-species comparison. *Front. Cell. Neurosci.* **2017**, *11*, 65. [CrossRef] [PubMed]

46. Goldsmith, P.; Harris, W.A. The zebrafish as a tool for understanding the biology of visual disorders. *Semin. Cell Dev. Biol.* **2003**, *14*, 11–18. [CrossRef] [PubMed]

47. Collery, R.F.; Cederlund, M.L.; Smyth, V.A.; Kennedy, B.N. Applying Transgenic Zebrafish Technology to Study the Retina. *Adv. Exp. Med. Biol.* **2006**, *572*, 201–207. [PubMed]

48. Gross, J.M.; Perkins, B.D. Zebrafish mutants as models for congenital ocular disorders in humans. *Mol. Reprod. Dev. Inc. Gamete Res.* **2008**, *75*, 547–555. [CrossRef] [PubMed]

49. Germana, A.; Catania, S.; Cavallaro, M.; González-Martínez, T.; Ciriaco, E.; Hannestad, J.; Vega, J. Immunohistochemical localization of BDNF-, TrkB-and TrkA-like proteins in the teleost lateral line system. *J. Anat.* **2002**, *200*, 477–485. [CrossRef] [PubMed]

50. Eichenbaum, J.W.; Cinaroglu, A.; Eichenbaum, K.D.; Sadler, K.C. A zebrafish retinal graded photochemical stress model. *J. Pharmacol. Toxicol. Methods* **2009**, *59*, 121–127. [CrossRef] [PubMed]

51. Zhang, N.; He, X.; Xing, Y.; Yang, N. Differential susceptibility of retinal ganglion cell subtypes against neurodegenerative diseases. *Graefe's Arch. Clin. Exp. Ophthalmol.* **2022**, *260*, 1807–1821. [CrossRef]

52. Núñez-Álvarez, C.; Osborne, N.N. Blue light exacerbates and red light counteracts negative insults to retinal ganglion cells in situ and R28 cells in vitro. *Neurochem. Int.* **2019**, *125*, 187–196. [CrossRef]

53. Núñez-Álvarez, C.; Suárez-Barrio, C.; del Olmo Aguado, S.; Osborne, N.N. Blue light negatively affects the survival of ARPE19 cells through an action on their mitochondria and blunted by red light. *Acta Ophthalmol.* **2019**, *97*, e103–e115. [CrossRef]

54. Sánchez-Ramos, C.; Bonnin-Arias, C.; Guerrera, M.C.; Calavia, M.; Chamorro, E.; Montalbano, G.; López-Velasco, S.; López-Muñiz, A.; Germanà, A.; Vega, J.A. Light regulates the expression of the BDNF/TrkB system in the adult zebrafish retina. *Microsc. Res. Tech.* **2013**, *76*, 42–49. [CrossRef] [PubMed]

55. Bilotta, J.; Saszik, S. The zebrafish as a model visual system. *Int. J. Dev. Neurosci.* **2001**, *19*, 621–629. [CrossRef]

56. Ganzen, L.; Venkatraman, P.; Pang, C.P.; Leung, Y.F.; Zhang, M. Utilizing Zebrafish Visual Behaviors in Drug Screening for Retinal Degeneration. *Int. J. Mol. Sci.* **2017**, *18*, 1185. [CrossRef] [PubMed]

57. Montalbano, G.; Levanti, M.; Mhalhel, K.; Abbate, F.; Laurà, R.; Guerrera, M.C.; Aragona, M.; Germanà, A. Acid-Sensing Ion Channels in Zebrafish. *Animals* **2021**, *11*, 2471. [CrossRef] [PubMed]

58. Germanà, A.; Sánchez-Ramos, C.; Guerrera, M.C.; Calavia, M.; Navarro, M.; Zichichi, R.; García-Suárez, O.; Pérez-Piñera, P.; Vega, J.A. Expression and cell localization of brain-derived neurotrophic factor and TrkB during zebrafish retinal development. *J. Anat.* **2010**, *217*, 214–222. [CrossRef]

59. Thomas, J.L.; Nelson, C.M.; Luo, X.; Hyde, D.R.; Thummel, R. Characterization of multiple light damage paradigms reveals regional differences in photoreceptor loss. *Exp. Eye Res.* **2012**, *97*, 105–116. [CrossRef] [PubMed]

60. Thummel, R.; Enright, J.M.; Kassen, S.C.; Montgomery, J.E.; Bailey, T.J.; Hyde, D.R. Pax6a and Pax6b are required at different points in neuronal progenitor cell proliferation during zebrafish photoreceptor regeneration. *Exp. Eye Res.* **2010**, *90*, 572–582. [CrossRef]

61. Thummel, R.; Kassen, S.C.; Enright, J.M.; Nelson, C.M.; Montgomery, J.E.; Hyde, D.R. Characterization of Müller glia and neuronal progenitors during adult zebrafish retinal regeneration. *Exp. Eye Res.* **2008**, *87*, 433–444. [CrossRef] [PubMed]

62. Thummel, R.; Kassen, S.C.; Montgomery, J.E.; Enright, J.M.; Hyde, D.R. Inhibition of Müller glial cell division blocks regeneration of the light-damaged zebrafish retina. *Dev. Neurobiol.* **2008**, *68*, 392–408. [CrossRef]

63. Dong, W.; Teraoka, H.; Kondo, S.; Hiraga, T. 2, 3, 7, 8-tetrachlorodibenzo-p-dioxin induces apoptosis in the dorsal midbrain of zebrafish embryos by activation of arylhydrocarbon receptor. *Neurosci. Lett.* **2001**, *303*, 169–172. [CrossRef]

64. Ross, M.H.; Pawlina, W.; Barnash, T.; Calligaro, A.; Di Renzo, M.F. *Atlante di Istologia e Anatomia Microscopica*; CEA: Singapore, 2010.

65. Haley, T.L.; Pochet, R.; Baizer, L.; Burton, M.D.; Crabb, J.W.; Parmentier, M.; Polans, A.S. Calbindin D-28K immunoreactivity of human cone cells varies with retinal position. *Vis. Neurosci.* **1995**, *12*, 301–307. [CrossRef] [PubMed]

66. Chiquet, C.; Dkhissi-Benyahya, O.; Cooper, H.M. Calcium-binding protein distribution in the retina of strepsirhine and haplorhine primates. *Brain Res. Bull.* **2005**, *68*, 185–194. [CrossRef] [PubMed]

67. Celio, M.R. Calbindin D-28k and parvalbumin in the rat nervous system. *Neuroscience* **1990**, *35*, 375–475. [CrossRef] [PubMed]

68. Hwang, I.K.; Yoo, K.Y.; Kim, D.S.; Jung, J.Y.; Shin, M.C.; Seo, K.; Kim, K.S.; Kang, T.C.; Won, M.H. Comparative Study on Calretinin Immunoreactivity in Gerbil and Rat Retina. *Anat. Histol. Embryol.* **2005**, *34*, 129–131. [CrossRef]

69. Nag, T.C.; Wadhwa, S. Developmental expression of calretinin immunoreactivity in the human retina and a comparison with two other EF-hand calcium-binding proteins. *Neuroscience* **1999**, *91*, 41–50. [CrossRef]

70. Nag, T.C.; Wadhwa, S. Calbindin and parvalbumin immunoreactivity in the developing and adult human retina. *Dev. Brain Res.* **1996**, *93*, 23–32. [CrossRef]

71. Lee, E.-S.; Lee, J.-Y.; Kim, G.H.; Jeon, C.-J. Identification of calretinin-expressing retinal ganglion cells projecting to the mouse superior colliculus. *Cell Tissue Res.* **2019**, *376*, 153–163. [CrossRef]

72. del Olmo-Aguado, S.; Núñez-Álvarez, C.; Osborne, N.N. Red light of the visual spectrum attenuates cell death in culture and retinal ganglion cell death in situ. *Acta Ophthalmol.* **2016**, *94*, e481–e491. [CrossRef]

73. Hamano, K.; Kiyama, H.; Emson, P.C.; Manabe, R.; Nakauchi, M.; Tohyama, M. Localization of two calcium binding proteins, calbindin (28 kD) and parvalbumin (12 kD), in the vertebrate retina. *J. Comp. Neurol.* **1990**, *302*, 417–424. [CrossRef]

74. Pochet, R.; Pasteels, B.; Seto-ohshima, A.; Bastianelli, E.; Kitajima, S.; Van Eldik, L.J. Calmodulin and calbindin localization in retina from six vertebrate species. *J. Comp. Neurol.* **1991**, *314*, 750–762. [CrossRef]

75. Zhang, C.; Wang, J.; Zhou, A.; Ye, Q.; Feng, Y.; Wang, Z.; Wang, S.; Xu, G.; Zou, J. Species-specific effect of microplastics on fish embryos and observation of toxicity kinetics in larvae. *J. Hazard. Mater.* **2021**, *403*, 123948. [CrossRef] [PubMed]

76. Pöstyéni, E.; Szabadfi, K.; Sétáló, G.; Gabriel, R. A Promising Combination: PACAP and PARP Inhibitor Have Therapeutic Potential in Models of Diabetic and Hypertensive Retinopathies. *Cells* **2021**, *10*, 3470. [CrossRef] [PubMed]

77. Sharma, R.K.; O'Leary, T.E.; Fields, C.M.; Johnson, D.A. Development of the outer retina in the mouse. *Dev. Brain Res.* **2003**, *145*, 93–105. [CrossRef] [PubMed]

78. Zhang, R.; Zhang, X.; Hu, F.; Wu, J. Fine structure of the human retina defined by confocal microscopic immunohistochemistry. *Br. J. Biomed. Sci.* **2021**, *78*, 28–34. [CrossRef]

79. Kovács-Öller, T.; Raics, K.; Orbán, J.; Nyitrai, M.; Völgyi, B. Developmental changes in the expression level of connexin36 in the rat retina. *Cell Tissue Res.* **2014**, *358*, 289–302. [CrossRef]

80. Nivison-Smith, L.; Khoo, P.; Acosta, M.L.; Kalloniatis, M. Pre-treatment with vinpocetine protects against retinal ischemia. *Exp. Eye Res.* **2017**, *154*, 126–138. [CrossRef]

81. Fu, Z.; Nian, S.; Li, S.-Y.; Wong, D.; Chung, S.K.; Lo, A.C.Y. Deficiency of aldose reductase attenuates inner retinal neuronal changes in a mouse model of retinopathy of prematurity. *Graefe's Arch. Clin. Exp. Ophthalmol.* **2015**, *253*, 1503–1513. [CrossRef]

82. Gábriel, R.; Erdélyi, F.; Szabó, G.; Lawrence, J.J.; Wilhelm, M. Ectopic transgene expression in the retina of four transgenic mouse lines. *Brain Struct. Funct.* **2016**, *221*, 3729–3741. [CrossRef]

83. Lee, S.C.S.; Weltzien, F.; Madigan, M.C.; Martin, P.R.; Grünert, U. Identification of AII amacrine, displaced amacrine, and bistratified ganglion cell types in human retina with antibodies against calretinin. *J. Comp. Neurol.* **2016**, *524*, 39–53. [CrossRef]

84. Uesugi, R.; Yamada, M.; Mizuguchi, M.; Baimbridge, K.G.; Kim, S.U. Calbindin D-28k and parvalbumin immunohistochemistry in developing rat retina. *Exp. Eye Res.* **1992**, *54*, 491–499. [CrossRef]

85. Trost, A.; Schroedl, F.; Marschallinger, J.; Rivera, F.J.; Bogner, B.; Runge, C.; Couillard-Despres, S.; Aigner, L.; Reitsamer, H.A. Characterization of dsRed2-positive cells in the doublecortin-dsRed2 transgenic adult rat retina. *Histochem. Cell Biol.* **2014**, *142*, 601–617. [CrossRef] [PubMed]

86. Kovács-Valasek, A.; Pöstyéni, E.; Dénes, V.; Mester, A.; Sétáló Jr, G.; Gábriel, R. Age-Related Alterations of Proteins in Albino Wistar Rat Retina. *Cells Tissues Organs* **2021**, *210*, 135–150. [CrossRef]

87. Ho, T.; Vessey, K.A.; Fletcher, E.L. Immunolocalization of the P2X4 receptor on neurons and glia in the mammalian retina. *Neuroscience* **2014**, *277*, 55–71. [CrossRef] [PubMed]

88. Zhang, W.; Li, C.; Guo, M. Use of ecofriendly alternatives for the control of bacterial infection in aquaculture of sea cucumber *Apostichopus japonicus*. *Aquaculture* **2021**, *545*, 737185. [CrossRef]

89. Vistamehr, S.; Tian, N. Light deprivation suppresses the light response of inner retina in both young and adult mouse. *Vis. Neurosci.* **2004**, *21*, 23–37. [CrossRef]

90. Emran, F.; Rihel, J.; Adolph, A.R.; Dowling, J.E. Zebrafish larvae lose vision at night. *Proc. Natl. Acad. Sci. USA* **2010**, *107*, 6034–6039. [CrossRef]

91. Xu, W.; Zhu, Q.; Liu, S.; Dai, X.; Zhang, B.; Gao, C.; Gao, L.; Liu, J.; Cui, Y. Calretinin Participates in Regulating Steroidogenesis by PLC-Ca2+-PKC Pathway in Leydig Cells. *Sci. Rep.* **2018**, *8*, 7403. [CrossRef]

92. Osborne, N.N.; Larsen, A.K. Antigens Associated with Specific Retinal Cells are Affected by Ischaemia Caused by Raised Intraocular Pressure: Effect of Glutamate Antagonists **Part of the work reported in this original communication was presented at the symposium entitled Excitatory Amino Acid Signaling, which was held in Kyoto, Japan, 15–18 July 1995 (organised by Y. Yoneda and M. Toru). Dr Yoneda also acted as executive editor in the processing of this manuscript. *Neurochem. Int.* **1996**, *29*, 263–270. [CrossRef]

93. Chun, M.-H.; Kim, I.-B.; Ju, W.-K.; Kim, K.-Y.; Lee, M.-Y.; Joo, C.-K.; Chung, J.-W. Horizontal cells of the rat retina are resistant to degenerative processes induced by ischemia-reperfusion. *Neurosci. Lett.* **1999**, *260*, 125–128. [CrossRef]

94. García-Suárez, O.; Pérez-Pérez, M.; Germanà, A.; Esteban, I.; Germanà, G. Involvement of growth factors in thymic involution. *Microsc. Res. Tech.* **2003**, *62*, 514–523. [CrossRef]

95. Germanà, A.; Guerrera, M.C.; Laurà, R.; Levanti, M.; Aragona, M.; Mhalhel, K.; Germanà, G.; Montalbano, G.; Abbate, F. Expression and Localization of BDNF/TrkB System in the Zebrafish Inner Ear. *Int. J. Mol. Sci.* **2020**, *21*, 5787. [CrossRef] [PubMed]

96. García-Suárez, O.; Germanà, A.; Hannestad, J.; Pérez-Pérez, M.; Esteban, I.; Naves, F.J.; Vega, J.A. Changes in the expression of the nerve growth factor receptors TrkA and p75LNGR in the rat thymus with ageing and increased nerve growth factor plasma levels. *Cell Tissue Res.* **2000**, *301*, 225–234. [CrossRef] [PubMed]

97. Abbate, F.; Guerrera, M.C.; Montalbano, G.; De Carlos, F.; Suárez, A.Á.; Ciriaco, E.; Germanà, A. Morphology of the european sea bass (*Dicentrarchus labrax*) tongue. *Microsc. Res. Tech.* **2012**, *75*, 643–649. [CrossRef] [PubMed]

98. Lauriano, E.; Guerrera, M.; Laurà, R.; Capillo, G.; Pergolizzi, S.; Aragona, M.; Abbate, F.; Germanà, A. Effect of light on the calretinin and calbindin expression in skin club cells of adult zebrafish. *Histochem. Cell Biol.* **2020**, *154*, 495–505. [CrossRef]

99. Aragona, M.; Porcino, C.; Guerrera, M.C.; Montalbano, G.; Laurà, R.; Levanti, M.; Abbate, F.; Cobo, T.; Capitelli, G.; Calapai, F.; et al. Localization of BDNF and Calretinin in Olfactory Epithelium and Taste Buds of Zebrafish (*Danio rerio*). *Int. J. Mol. Sci.* **2022**, *23*, 4696. [CrossRef]

100. Alesci, A.; Capillo, G.; Fumia, A.; Messina, E.; Albano, M.; Aragona, M.; Lo Cascio, P.; Spanò, N.; Pergolizzi, S.; Lauriano, E.R. Confocal Characterization of Intestinal Dendritic Cells from Myxines to Teleosts. *Biology* **2022**, *11*, 1045. [CrossRef]